Biosensors and Bioelectronics 117 (2018) 508–514

Contents lists available at ScienceDirect

Biosensors and Bioelectronics

journal homepage: www.elsevier.com/locate/bios

Ultra-sensitive electrochemical detection of oxidative stress biomarker 8-hydroxy-2′-deoxyguanosine with poly (L-arginine)/graphene wrapped Au nanoparticles modified electrode

M.Z.H. Khan[a,c], Xiaoqiang Liu[a], Yunfei Tang[a], Xiuhua Liu[a,b,*]

[a] College of Chemistry and Chemical Engineering, Henan University, China
[b] Key Laboratory of Natural Medicine and Immune-Engineering of Henan Province, Kaifeng 475004, Henan, China
[c] Dept. of Chemical Engineering, Jessore University of Science and technology, Jessore 7408, Bangladesh

ARTICLE INFO

Keywords:
Electrochemical biosensor
Poly (L-arginine), reduced graphene oxide
Gold nanoparticle
8-OHdG, cancer biomarker

ABSTRACT

An innovative electrochemical sensor assembly relying on a simple “green” electrochemical reduction route is presented for the sensitive detection of 8-hydroxy-2′-deoxyguanosine (8-OHdG), the most abundant oxidative product of DNA. The sensing film consisted of poly (L-arginine) and graphene wrapped Au nanoparticles was fabricated on glassy carbon electrode (GCE/P-Arg/ErGO-AuNPs) using subsequent ‘layer-by-layer’ regime through electrochemical technique. The proposed method was also successfully applied for the quantification of 8-OHdG in the presence of interfering biomolecules like ascorbic acid and uric acid. Scanning electron microscopy (SEM) was utilized to characterize the surface morphology of the composite electrode. Electrochemical characterizations of the bare and modified electrodes were carried out via cyclic voltammetry (CV) and electrochemical impedance spectroscopy (EIS). According to differential pulse voltammetry (DPV) results, there were linear relationships between the peak currents and the concentrations in the ranges of 1.0–100 nM (R^2 = 0.996), and 0.5–10 μM (R^2 = 0.990), with a detection limit (S/N = 3) of 1.0 nM. Furthermore, the proposed sensor was successfully applied for the determination of target analyte in human urine samples and a very high recovery percentage was obtained.

1. Introduction

8-hydroxy-2′-deoxyguanosine (8-OHdG) is an important biomarker and one of the major products of oxidative DNA damage, produced by the attack of reactive oxygen species (ROS) at the eighth carbon atom of guanine base (Martins et al., 2017) (Scheme 1). The higher concentrations of 8-OHdG in body fluids is typically correlated with human hepatocarcinogenesis (Shimoda et al., 1994), various cancers (Bialkowski et al., 1996), neurological disorders (Chen et al., 2009), diabetes (Nishikawa et al., 2003), and aging (Tamae et al., 2009). Therefore, the analysis of 8-OHdG in human fluid is extremely important to measure its level in patients suffering from the above-stated diseases and also for the assessment of an individual's cancer risk or the exposure to various carcinogens (Li et al., 2007).

So far, various techniques have been employed to quantitative analysis of 8-OHdG in biological samples, including high performance liquid chromatography with electrochemical detection (HPLC-ECD) (Saravanabhavan et al., 2010), gas chromatography-mass spectrometry (GC-MS) (Lin et al., 2004), high performance capillary electrophoresis (HPCE) (Weiss and Lunte, 2000) and post labelling method (Maatouk et al., 2004). Nevertheless, the requirement of sophisticated and laborious technologies, long response time and high cost of analysis limit those techniques applicability. Unlike conventional techniques, several biosensing devices have been reported in the literature based on the electrochemical oxidation activity of 8-OHdG as it undergoes oxidation via a two-electron and two-proton charge transfer reaction (Jia et al., 2018; Kumar et al., 2017a; Li et al., 2007; Martins et al., 2017, 2016; Shahzad et al., 2017a; Shang et al., 2018a; Yang et al., 2015a). However, most of these electrodes demonstrated the low sensitivity and low selectivity and were not explored in biological fluids. It is well known that, ascorbic acid (AA) and uric acid (UA) are the main interferents in the determination of 8-OHdG in biological fluids (Jia and Wang, 2013a) due to their similar electrochemical response. Therefore, sensitive determination of trace amount of 8-OHdG in complex matrix like urine is still a challenge and thus calls for more intense research.

In recent years, poly (L–arginine) modified electrode has attracted significant attention which can be easily electropolymerized on electrode surface through combination of -NH_2 and -COOH (Tığ, 2017; Yi

* Corresponding author at: College of Chemistry and Chemical Engineering, Henan University, China.
E-mail address: liuxiuhua@henu.edu.cn (X. Liu).

https://doi.org/10.1016/j.bios.2018.06.048
Received 1 June 2018; Accepted 24 June 2018
Available online 26 June 2018
0956-5663/

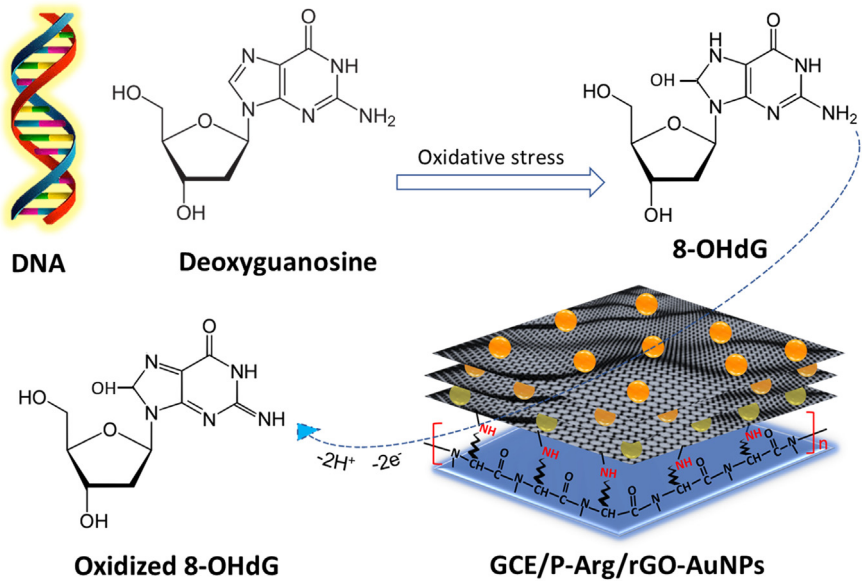

Scheme 1. Formation and electrochemical detection mechanism of 8-OHdG biomarker with GCE/P-Arg/ErGO-AuNPs modified electrode.

et al., 2016; Zhou et al., 2015). Such polymer films can notably improve the stability of the electrode response and improve the electroactivity properties of analytes. Several researchers combined graphene oxide (GO) and polymer composites to improve the electrocatalytic performance of the electrodes (Devadas et al., 2014; Hasanzadeh et al., 2017; Tığ, 2017). Owing to the two-dimensional (2D) honeycomb lattice, GO based materials with tunable oxygen functionalities on their basal plane provide an effective sensing platform for pursuing experiments in selective detection of bio-entities (Khan, 2017; Khan et al., 2017a, 2017b). Au-nanoparticles (AuNPs) decorated graphene oxides are one of the most studied and widely employed materials in electrochemical sensing (Khalil et al., 2016). Graphene with nanoparticles provide additional synergistic properties by improving electron mobility, electrical conductivity, as well as increasing surface area for analyte binding (Otari et al., 2017). The incorporation of AuNPs into graphene not only prevent restacking and agglomeration of the graphene sheets during reduction process but also enhance the achievable selectivity and sensitivity of the sensing platform. Recently, Zhang et al. also reported that rGO/AuNPs composite shows better catalytic activities than AuNPs/GO composite or free AuNPs (Huang et al., 2010).

In this work, a novel electrochemical sensor was proposed for the first time based on the advantages of polymer, reduced graphene oxide-metal nanoparticles nanocomposite film modified glassy carbon electrode (GCE/P-Arg/ErGO-AuNPs) for the determination of 8-OHdG in the presence of AA and UA. The electrocatalytic activity of the different modified electrodes was also evaluated. Furthermore, the potential application of the modified electrode for sensing these compounds in human urine samples was also investigated.

2. Materials and methods

2.1. Reagents

L-arginine, 8-Hydroxy-2′-deoxyguanosine (8-OHdG), L-Ascorbic acid, uric acid Tetrachloroaurate ($HAuCl_4$) trihydrate were purchased from Sigma Aldrich, China. Graphene nanosheet was produced from natural graphite powder by a modified Hummers method and it was kindly supplied by Prof. Yuta Nishina, Japan. The detail of GO nanosheet preparation was described in previous report (Morioku et al., 2016) and in Supporting Information (SI). All the reagents for GO nanosheet preparation were purchased from Sigma Aldrich. The solutions of analytes were prepared daily by dissolving the required amount of reagent in 0.1 M PBS (pH 7.4). A redox probe solution was prepared in 0.1 mol L^{-1} KCl, which contained 5.0 mmol L^{-1} Fe $(CN)_6^{3-}$ and 5.0 mmol L^{-1} Fe $(CN)_6^{4-}$. All of the chemicals used in this work were of analytical grade and used without purification.

2.2. Preparation of GCE/P-Arg/ErGO-AuNPs nanocomposite electrode

The sequential 'layer-by-layer' film was fabricated on a GCE with a diameter of 3 mm by cyclic voltammetry (CV). Prior to modification, the GCE electrode was polished to a mirror finish using a 0.05 μm alumina slurry, after which it was sonicated in nitric acid (1:1), ethanol, and deionized water. Next, the electrode was rinsed with ultra-pure water and allowed to dry under N_2. The cleaned GCE was dipped into 0.1 M PBS (pH 7.4) containing 2.5 mM L-Arg and cyclic voltammetry (CV) was performed in the potential range from -2.2 to 2.0 V at 100 mVs^{-1} for definite cycles. After electropolymerization, the GCE/P-Arg electrode was carefully washed with ultrapure water and dried in air. To prepare GCE/P-Arg/ErGO-AuNPs film, 0.5 mg mL^{-1} GO was dispersed in 0.1 M PBS (pH 7.4) solution in nanosheet form and was stirred and sonicated for 15 min and 1 h respectively. Later, 0.5 mM $HAuCl_4$ solution was added during sonication of GO. The GO-AuNPs nanocomposite was electrodeposited on GCE/P-Arg electrode under deoxygenated conditions (guaranteed via nitrogen bubbling) through a series of 15 cyclic voltammetries between − 1.2 and 0.7 V vs. Ag/AgCl and at a scan rate of 50 mV s^{-1}. After electrochemical reduction of GO (ErGO) and simultaneously electrodeposition of ErGO-AuNPs, the modified electrode GCE/P-Arg/ErGO-AuNPs was washed with ultrapure water, and then air-dried and stored in 4 °C for use. For electrode characterization and comparison, four different electrodes were also prepared with or without P-Arg, ErGO, and AuNPs respectively.

2.3. Apparatus

Electrochemical measurements were carried out using CHI electrochemical workstation (Shanghai CH Instruments). A conventional three electrode system was used for electrochemical performance. GCE with a surface area of 3 mm was used as the working electrode, Ag|AgCl electrode as the reference electrode and platinum wire as the counter electrode. Scanning electron microscopy (SEM) was performed using Hitachi S-3000H model and electrochemical impedance spectroscopy (EIS) studies were analyzed using ZAHNER impedance analyzer EIM6ex ZAHNER (Kroanch, Germany). All electrochemical measurements were

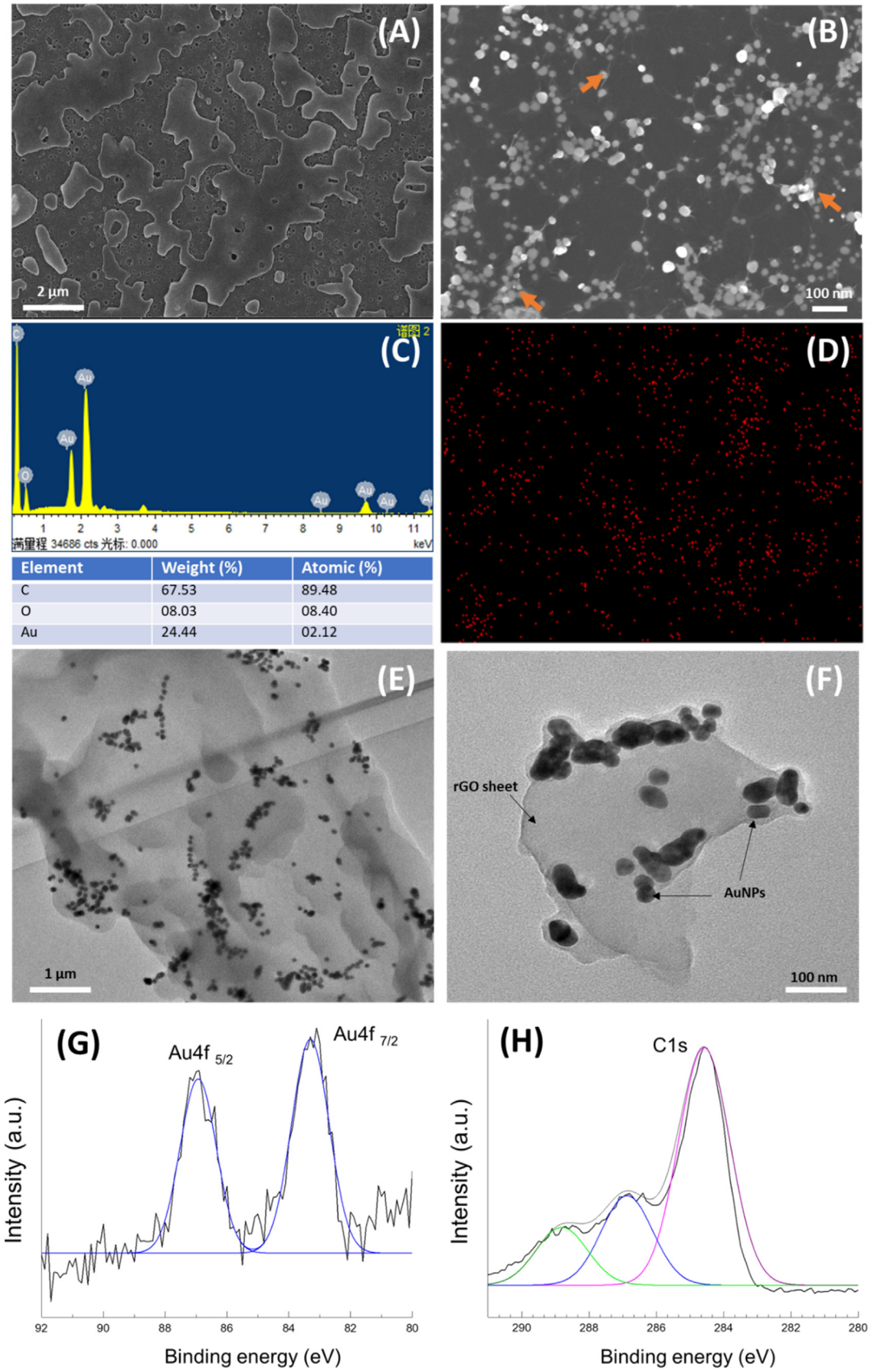

Element	Weight (%)	Atomic (%)
C	67.53	89.48
O	08.03	08.40
Au	24.44	02.12

Fig. 1. SEM images of (A) GCE/P-Arg film, and (B) GCE/P-Arg/ErGO-AuNPs nanocomposite film. The arrow marks indicate the wrapping of AuNPs by GO nanosheet. (C) The EDX spectrum of the nanocomposite film, and (D) their corresponding element mapping showing the distribution of Au nanoparticles on GCE/P-Arg/ErGO-AuNPs nanocomposite film. Low (E) and high (F) resolution TEM images of ErGO-AuNPs nanocomposite. Survey and high resolution XPS spectra of ErGO-AuNPs nanocomposite film: (G) spectrum of Au 4f pattern, and (H) high resolution C 1s spectrum with fitted curves.

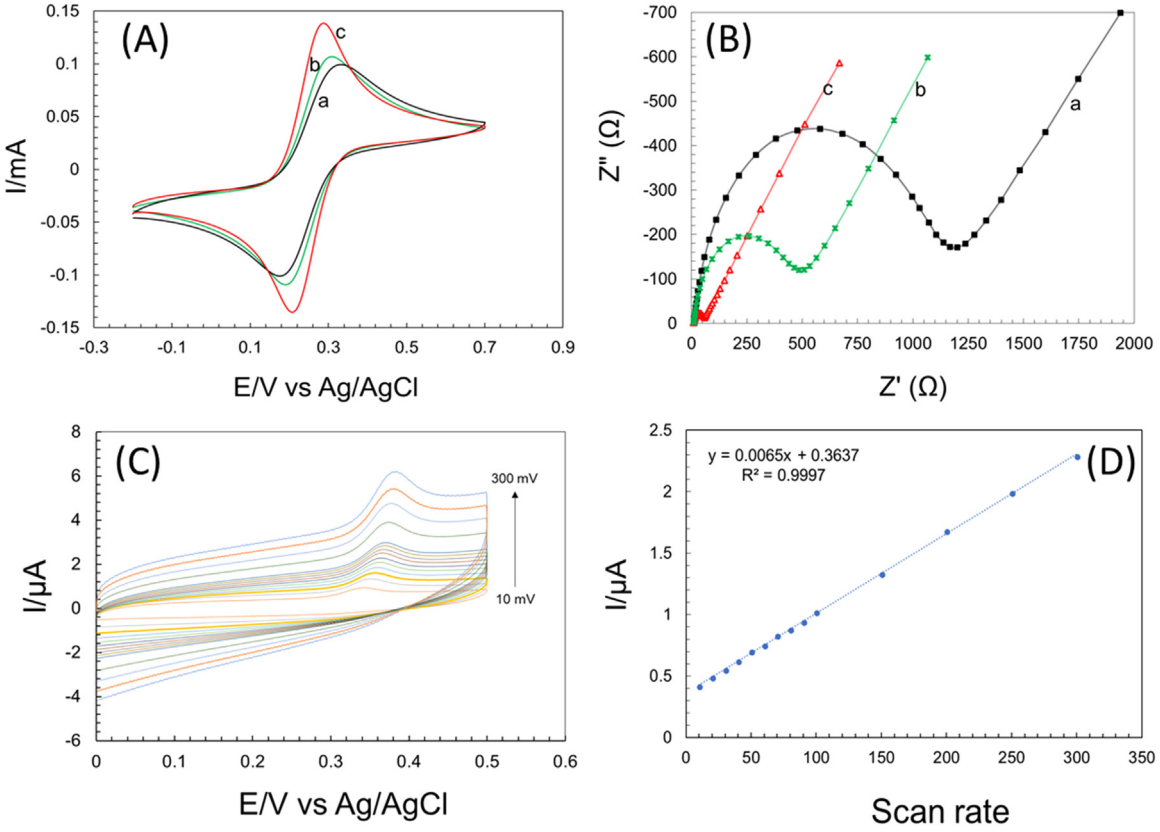

Fig. 2. Cyclic voltammograms (A) and Nyquist plot of EIS (B) of the different electrodes measured in 0.1 M L^{-11} KCl including 5.0 mM L^{-11} $Fe(CN)_6^{3-1/4-1}$: (a) bare GCE, (b) GCE/P-Arg, and (c) GCE/P-Arg/ErGO-AuNPs nanocomposite film. CVs of modified electrode in 0.1 M PBS (pH 7.0) solution with 0.1 μM 8-OHdG measured at different scan rates (10–300 mV/s) (C), and the corresponding calibration plots between the anodic and cathodic peak currents with the scan rate (D).

carried out at room temperature and electrolyte solutions were kept under nitrogen (N_2) atmosphere.

3. Results and discussion

3.1. Layer-by-layer electrochemical modification of electrode

The details of the observations during electrochemical depositions were descried in Supporting Information (SI). The electropolymerization of L-arginine was performed by cyclic sweeping from − 2.3 to 2.0 V at 100 mV/s for fifteen cycles in 0.1 M PBS containing 2.5 mM L-Arginine solution at pH 7.4. Fig. SI-1 shows the continuous cyclic voltammograms of electrochemical polymerization of P-Arg on the surface of GCE. The formation of polymer film on the bare GCE electrode surface was confirmed with the increasing of peak current with the number of CV cycles (Zhou et al., 2015). The monomer L-Arginine oxidizes at high positive potential and forms α-amino acid free radical that stimulates the polymerization. The resulted poly (L-Arginine) or P-Arg contains more amino than carboxyl and can directly linked on the electrode surface by the formation of covalent bond (C-N) as shown in Fig. 1A. To the best of our knowledge, this is the first-time observation of clear P-Arg film electrodeposition on GCE with regular and patterned interconnected net-like structure. The observed surface morphology indicates that P-Arg film has been successfully adhered to the electrode surface.

We adopted an electrochemical technique for the simultaneous reduction of GO and its co-electrodeposition along with nano Au (AuNPs) without reducing agents onto the electrode surface using cyclic voltammetry. For electrodeposition of ErGO-AuNPs composite, a dispersion containing 0.5 mg mL^{-1} GO and 0.1 mM $HAuCl_4$ was prepared. The details of the GO nanosheet preparation and the formation of graphene wrapped AuNPs has been described in SI. The CV electrodeposition was performed in the dispersion after N_2 bubbling for 10 min, which was performed between − 1.2 and 0.7 V at a sweep rate of 50 mV s^{-1} for 15 potential cycles.

The formation of ErGO nanosheet was confirmed by several measurements and reported in our previous work (Khan et al., 2018). The increase in the peak currents with successive potential scans confirms the electrodeposition of conductive film over the electrode that increased with every new cycle. This process is responsible for simultaneous reduction/electrodeposition of nonconductive GO and AuNPs into electrochemically-reduced GO (ErGO) wrapped AuNPs, which is very stable due to its poor solubility in common solvents (Morioku et al., 2016). As shown in Fig. 1B, AuNPs with an average size of ~ 25 nm uniformly and densely wrapped with the ErGO film. The size of AuNPs and its homogeneous distribution throughout ErGO film depends not only on the concentration of GO and AuNPs solution, but also on the number of the deposition cycle and scan rate. For the details of the optimum conditions, please see Supporting Information (Fig. Si-3). To the best of our knowledge, the clear wrapping of AuNPs with several layers of ErGO nanosheets is observed for the first time. The TEM images (Fig. 1E, F) are very much consistant with SEM findings and prove the clear wrapping of AuNPs with ErGO sheets.

To investigate the structural evolution of electrochemically deposited ErGO-AuNPs nanocomposite, XPS measurement was done and shown in Fig. 1g, h. High resolution Au 4f peaks (Au $4f_{5/2}$ and Au $4f_{7/2}$ spin-orbit doublets) were observed from ErGO-AuNPs nanocomposite modified electrode which are centered at ~ 83.5 and ~ 87.0 eV respectively. The characteristics and chemical nature of gold within the nanocomposite has been attributed as metallic Au° (after reduction of Au^{3+} to Au°) as suggested by other researchers as well (Kar et al., 2016). Moreover, compared with standard referencing position of

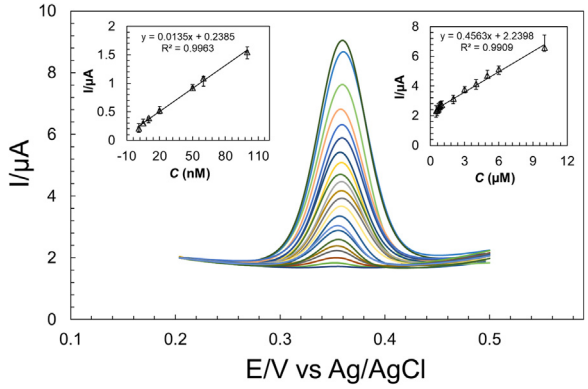

Fig. 3. DPVs obtained for determination of 8-OHdG using GCE/P-Arg/ErGO/AuNPs electrode in pH 7.4 phosphate buffer at scan rate of 50 mV/s with a wide range of concentrations from 0.1 nM to 10 μM. All the inset shows the corresponding calibration curves for high and low concentrations.

metallic Au°, the observed negative shift of ~ 0.6 eV reveals the strong interaction between ErGO and AuNPs (Li et al., 2012). Fig. 1g represents the high resolution XPS spectra of C 1s region with clear binding arrangement of C-O inside the nanocomposite film. Gaussian–Lorentzian peak shape was used to resolve the C 1s curve fitting. Three well defined peaks centered at ~ 284.66, ~ 286.70, and ~ 288.3 eV have been assigned to C=C/C–C, C–O, and C=O respectively. The high atom ratio of C/O indicates the deoxygenation during electrochemical reduction process.

3.2. Electrochemical characterization of GCE/P-Arg/ErGO-AuNPs nanocomposite electrode

The electrochemical characterization of the bare and modified electrodes was performed via CV and EIS in 0.1 M L^{-1} KCl including 5.0 mM L^{-1} $Fe(CN)_6^{3-/4-}$. A pair of well-defined redox peaks corresponding to $Fe(CN)_6^{3-/4-}$ appeared with the lowest peak currents at the bare GCE. The peak to peak separation (ΔEp) value was calculated as 254 mV, 185 mV, and 95 mV for bare GCE, GCE/P-Arg, and GCE/P-Arg/ErGO-ANPs electrode respectively (Fig. 2A). The positive charges of P-Arg facilitates the electrochemical reaction of $Fe(CN)_6^{3-/4-}$ as reported by earlier researchers (Hasanzadeh et al., 2017; Tığ, 2017). An obvious increased redox current and a decreased potential difference were observed after modification with ErGO and AuNPs nanocomposite. The possible reason may be ascribed to that the conductive graphene sheets connected individual AuNPs that effectively facilitated fast electron transfer between the modifying layer and GCE substrate, thus resulting in synergetic signal amplification. Therefore, the results demonstrated that GCE/P-Arg/ErGO-AuNPs with excellent electro-catalytic prosperities were designed.

We have also calculated the electrochemical active surface area (A) for bare and modified electrodes based on the Randles–Sevcik equation (Du et al., 2014).

$$I_p = 2.69 \times 10^5 A D^{1/2} n^{3/2} \gamma^{1/2} C \quad (1)$$

where A is the electroactive surface area, D is the diffusion coefficient of the molecule (equal to $6.70 \pm 0.02 \times 10^{-6}$ cm^2/s), C is the concentration of the probe molecule in the solution (mol/cm^3), n is the number of electrons in the redox reaction, γ is the scan rate (V/s). The calculated A value for the GCE, GCE/P-Arg, and GCE/P-Arg/ErGO-AuNPs were 0.089 cm^2, 0.142 cm^2, and 0.312 cm^2 respectively. This finding proved that GCE/P-Arg/ErGO-AuNPs modified electrode has the maximum electrochemical active surface area and high electron transfer kinetics.

Electrochemical impedance spectroscopy (EIS) experiments were performed to confirm the synergy between various modified electrodes and the results were shown in Fig. 2B. It could be easily observed that the bare GCE shows the largest semicircle appeared with a R_{ct} of 1089 Ω, showing the lowest transfer rate. Whereas GCE/P-Arg modified electrode shows a R_{ct} value of 441 Ω. When the electrode is modified by ErGO-AuNPs nanocomposite, the diameter of semicircle obviously decreases (R_{ct} value of 115 Ω) owing to the high electrical conductivity, thereby promoting a higher electron transfer rate in the redox probe. Moreover, the relationship between different scan rate and peak current was also studied to investigate the electrochemical mechanism of proposed electrode. A linear relationship with good correlation coefficients was found between the peak current values and the scan rate as shown in the inset of figure., which suggesting that the mass transfer phenomenon is an adsorption-controlled process at the solution-electrode interface.

Fig. 2c represents the CV behavior of GCE/P-Arg/ErGO-AuNPs modified electrode toward 8-OHdG detection at different scan rates. A well-defined oxidation peak was observed at + 0.36 V which gradually shifted toward positive values with the increasing of scan rate. As shown in Fig. 2d, the linear relationship between scan rate and anodic peak current suggest an adsorption-controlled electrochemical oxidation process which is in good agreement with other researcher as well (Martins et al., 2017).

3.3. Electrochemical detection of 8-OHdG

The electrochemical behavior of modified electrode in the presence of 8-OHdG was investigated by differential pulse voltammograms (DPV) in wide potential range. All experimental procedures were performed in 0.1 M PBS (pH 7.4) at room temperature. For all the DPV analysis, we have employed the following parameters: constant time interval of 90 s; N_2 gas purging into the electrolyte solution for 5 min before the start of each experiment; 50 mV for pulse amplitude, 0.05 ms for pulse width; and 200 ms for pulse period. Fig. 3 illustrates the DPVs for the individual detection of 8-OHdG and their calibration curves. As shown in Fig. 3, the change of DPVs indicates that the oxidative peak current (I_{pa}) has linear relationship with the concentration (C) of 8-OHdG. The calibration curve exhibits two linear segments in the range from 1.0 to 100 nM (R^2 = 0.996), and 0.5–10 μM (R^2 = 0.990), with a detection limit (S/N = 3) of 1.0 nM. Moreover, the analytical findings of this study were compared with several modified electrodes reported in last few years and presented in Table 1.

3.4. Selectivity, reproducibility, and stability study

Since the presence of high concentration of AA and UA in biological systems together with monoamine neurotransmitters, it should be taken into consideration before target analytes determination. From Fig. 4, it can be observed that well separated peaks corresponding to the oxidation of AA and UA were obtained at − 0.02 V, and 0.27 V respectively, along with the oxidation peak of 8-OHdG at 0.36 V. The calibration curve in the presence of those interference exhibits a linear segment in the range from 1.0 to 100 nM (R^2 = 0.994). Hence, it can be concluded that the proposed sensor has good selectivity towards the determination of 8-OHdG. Moreover, the peak of 8-OHdG did not exhibit any significant deviation even in the presence of physiological concentration of AA (1 mM), and UA (400 μM), which are commonly present in human biological fluids (Fig. SI-5).

A series of repetitive voltammetric measurements were carried out at the same GCE/P-Arg/ErGO-AuNPs nanocomposite electrode to evaluate the precision of this method. The relative standard deviations (R.S.D.) obtained for each 10 μM 8-OHdG measurements (n = 10) were 1.31%, 1.55% and 2.10% respectively, indicating an excellent detecting reproducibility. For stability test, the modified electrode was kept at 4 °C for 4 weeks and the peak current did not have an obvious change (lower than 7%) for the same concentration of 10 μM analyte solution, illustrating the good film stability of the proposed sensor.

Table 1
Comparison of the proposed method with other electrochemical methods recently reported (2013–2018) for the determination of 8-OHdG.

Electrode	Method	Linear range (μM)	LOD (nM)	Reference
SWCNTs-Nafion	DPV	0.03–1.25	8.0	(Yang et al., 2015b)
ER-GO/Nafion/GCE	DPV	0.07–33	1.12	(Jia and Wang, 2013b)
CNT-PEI/ GCE	DPV	0.5–30	100	(Gutiérrez et al., 2008)
DNA/P3MT /GCE	CV	0.02–19.6	56	(Wang et al., 2009)
MWCNT/ErGO/GCE	SWV	3–75	35	(Rosy and Goyal, 2016)
SrGO-HD/GCE	DPV	0.0020–20	1.0	(Shahzad et al., 2017b)
MIP Sensor	DPV	0.020–3	3.0	(Kumar et al., 2017b)
PSWNT/GCE	LSV	0.0029–87	0.99	(Shang et al., 2018b)
GCE/P-Arg/ErGO-AuNPs	DPV	0.001–0.1; 0.5–10	1.0	This work

SWCNTs: Single wall carbon nano tubes; GCE: Glassy carbon electrode; GNs: Graphene nanosheets (GNs); ER-GO: Electroreduction graphene oxide; CNT: Carbon nanotube; PEI: Polyethylenimine; P3MT: Poly(3-methylthiophene); SrGO: S-doped reduced graphene/glassy carbon electrode; PSWNT: Porous single-walled carbon nanotubes.

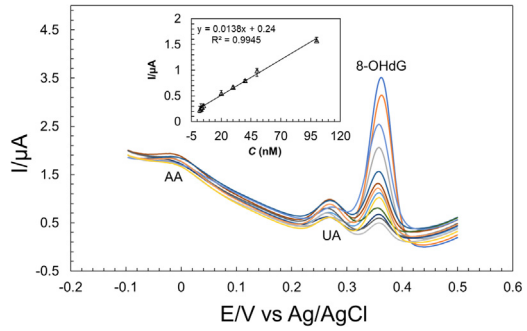

Fig. 4. DPVs of the determination of 8-OHdG (1–100 nM) in the presence of interference AA (400 μM) and UA (1 μM). Inset: corresponding calibration curves vs. concentrations of 8-OHdG.

3.5. Real sample analysis

To investigate the practicality of the proposed method, GCE/P-Arg/ErGO-AuNPs electrode was applied to the determination of 8-OHdG in healthy human urine using the standard addition method. The human urine samples were diluted 100 times using 0.1 M PBS (pH 7.4). The obtained recovery results ranged from 98.55% to 101.19% reveals the possibility of the proposed sensor for real biological samples. The recovery values were estimated and summarized in Supporting information Table 1 (SI-7).

4. Conclusion

In this present work, we have successfully prepared GCE/P-Arg/ErGO-AuNPs modified electrode via electrochemical deposition technique and investigated the electrochemical performance of proposed electrode towards the detection of 8-OHdG biomarker. The as-prepared nanocomposite modified electrode successfully resolved the overlapped voltammetric signals of target analyte and its interferences into well-separated peaks by the DPV method. In particular, the electrode showed wide linear concentration ranges (1.0–100 nM; 0.5–10 μM) between the peak current and 8-OHdG concentration with a detection limit of 1.0 nM. Additionally, the modified electrode shows applicability for the detection of these biological substance in human urine samples with high recovery values. Hence, the prepared GCE/P-Arg/ErGO-AuNPs sensor constitutes a promising low-cost approach for the analysis of 8-OHdG for diagnostic research. Further extensive studies are suggested on long-term biocompatibility of the proposed electrode and the interaction mechanism of ErGO-AuNPs hybrids with other complex biological fluids for point-to-care applications.

Acknowledgments

We are grateful for the financial support from the National Natural Science Foundation of China (21705033) and the Natural Science Foundation of Henan Provincial Science and Technology Department (162300410043, 182102410077).

Appendix A. Supplementary material

Supplementary data associated with this article can be found in the online version at http://dx.doi.org/10.1016/j.bios.2018.06.048.

References

Bialkowski, K., Kowara, R., Windorbska, W., Olinski, R., 1996. 8-Oxo-2′-deoxyguanosine level in lymphocytes DNA of cancer patients undergoing radiotherapy. Cancer Lett. 99, 93–97.

Chen, C.-M., Liu, J.-L., Wu, Y.-R., Chen, Y.-C., Cheng, H.-S., Cheng, M.-L., Chiu, D.T., 2009. Increased oxidative damage in peripheral blood correlates with severity of Parkinson's disease. Neurobiol. Dis. 33, 429–435. http://dx.doi.org/10.1016/j.nbd.2008.11.011.

Devadas, B., Cheemalapati, S., Chen, S.M., Ali, M.A., Al-Hemaid, F.M.A., 2014. Highly sensing graphene oxide/poly-arginine-modified electrode for the simultaneous electrochemical determination of buspirone, isoniazid and pyrazinamide drugs. Ionics (Kiel) 21, 547–555. http://dx.doi.org/10.1007/s11581-014-1179-z.

Du, J., Yue, R., Ren, F., Yao, Z., Jiang, F., Yang, P., Du, Y., 2014. Novel graphene flowers modified carbon fibers for simultaneous determination of ascorbic acid, dopamine and uric acid. Biosens. Bioelectron. 53, 220–224. http://dx.doi.org/10.1016/J.BIOS.2013.09.064.

Gutiérrez, A., Osegueda, S., Gutiérrez-Granados, S., Alatorre, A., García, M.G., Godínez, L.A., 2008. Amperometric detection and quantification of 8-Hydroxy-2′-deoxyguanosine (8-OHdG) using dendrimer modified electrodes. Electroanalysis 20, 2294–2300. http://dx.doi.org/10.1002/elan.200804324.

Hasanzadeh, M., Mokhtari, F., Shadjou, N., Eftekhari, A., Mokhtarzadeh, A., Jouyban-Gharamaleki, V., Mahboob, S., 2017. Poly arginine-graphene quantum dots as a biocompatible and non-toxic nanocomposite: layer-by-layer electrochemical preparation, characterization and non-invasive malondialdehyde sensory application in exhaled breath condensate. Mater. Sci. Eng. C 75, 247–258. http://dx.doi.org/10.1016/j.msec.2017.02.025.

Huang, J., Zhang, L., Chen, B., Ji, N., Chen, F., Zhang, Y., Zhang, Z., 2010. Nanocomposites of size-controlled gold nanoparticles and graphene oxide: formation and applications in SERS and catalysis. Nanoscale 2, 2733. http://dx.doi.org/10.1039/c0nr00473a.

Jia, L., Wang, H., 2013a. Electrochemical reduction synthesis of graphene/Nafion nanocomposite film and its performance on the detection of 8-hydroxy-2′-deoxyguanosine in the presence of uric acid. J. Electroanal. Chem. 705, 37–43. http://dx.doi.org/10.1016/j.jelechem.2013.07.013.

Jia, L., Wang, H., 2013b. Electrochemical reduction synthesis of graphene/Nafion nanocomposite film and its performance on the detection of 8-hydroxy-2′-deoxyguanosine in the presence of uric acid. J. Electroanal. Chem. 705, 37–43. http://dx.doi.org/10.1016/j.jelechem.2013.07.013.

Jia, L.P., Wang, L.J., Ma, R.N., Shang, L., Zhang, W., Xue, Q.W., Wang, H.S., 2018. An electrochemical aptasensor for the highly sensitive detection of 8-hydroxy-2′-deoxyguanosine based on the hybridization chain reaction. Talanta 179, 414–419. http://dx.doi.org/10.1016/j.talanta.2017.11.036.

Kar, P., Sardar, S., Liu, B., Sreemany, M., Lemmens, P., Ghosh, S., Pal, S.K., 2016. Facile synthesis of reduced graphene oxide–gold nanohybrid for potential use in industrial waste-water treatment. Sci. Technol. Adv. Mater. 17, 375–386. http://dx.doi.org/10.1080/14686996.2016.1201413.

Khalil, I., Julkapli, N.M., Yehye, W.A., Basirun, W.J., Bhargava, S.K., 2016. Graphene-gold nanoparticles hybrid-synthesis, functionalization, and application in a

electrochemical and surface-enhanced raman scattering biosensor. Materials. http://dx.doi.org/10.3390/ma9060406.
Khan, M.Z.H., 2017. Nanoparticles modified ITO based biosensor. J. Electron. Mater. 46, 2254–2268. http://dx.doi.org/10.1007/s11664-016-5172-3.
Khan, M.Z.H., Liu, X., Zhu, J., Ma, F., Hu, W., Liu, X., 2018. Electrochemical detection of tyramine with ITO/APTES/ErGO electrode and its application in real sample analysis. Biosens. Bioelectron. http://dx.doi.org/10.1016/J.BIOS.2018.02.042.
Khan, M.Z.H., Rahman, M.A., Yasmin, P., Tareq, F.K., Yuta, N., Komeda, T., Jahan, R.A., 2017a. Formation and characterization of copper nanocube-decorated reduced graphene oxide film. J. Nanomater. 2017. http://dx.doi.org/10.1155/2017/5702838.
Khan, M.Z.H., Shahed, S.M.F., Yuta, N., Komeda, T., 2017b. Deposition of an ultraflat graphene oxide nanosheet on atomically flat substrates. J. Electron. Mater. 46. http://dx.doi.org/10.1007/s11664-017-5327-x.
Kumar, N., Rosy, Goyal, R.N., 2017a. A melamine based molecularly imprinted sensor for the determination of 8-hydroxydeoxyguanosine in human urine. Talanta 166, 215–222. http://dx.doi.org/10.1016/j.talanta.2017.01.058.
Kumar, N., Rosy, Goyal, R.N., 2017b. A melamine based molecularly imprinted sensor for the determination of 8-hydroxydeoxyguanosine in human urine. Talanta 166, 215–222. http://dx.doi.org/10.1016/j.talanta.2017.01.058.
Li, J., Liu, C., Liu, Y., 2012. Au/graphene hydrogel: synthesis, characterization and its use for catalytic reduction of 4-nitrophenol. J. Mater. Chem. 22, 8426. http://dx.doi.org/10.1039/c2jm16386a.
Li, T.H., Jia, W.L., Wang, H.S., Liu, R.M., 2007. Electrochemical performance of 8-hydroxy-2′-deoxyguanosine and its detection at poly(3-methylthiophene) modified glassy carbon electrode. Biosens. Bioelectron. 22, 1245–1250. http://dx.doi.org/10.1016/j.bios.2006.05.005.
Lin, H.-S., Jenner, A.M., Ong, C.N., Huang, S.H., Whiteman, M., Halliwell, B., 2004. A high-throughput and sensitive methodology for the quantification of urinary 8-hydroxy-2′-deoxyguanosine: measurement with gas chromatography-mass spectrometry after single solid-phase extraction. Biochem. J. 380, 541–548. http://dx.doi.org/10.1042/BJ20040004.
Maatouk, I., Bouaïcha, N., Plessis, M.J., Périn, F., 2004. Detection by 32P-postlabelling of 8-oxo-7,8-dihydro-2′-deoxyguanosine in DNA as biomarker of microcystin-LR- and nodularin-induced DNA damage in vitro in primary cultured rat hepatocytes and in vivo in rat liver. Mutat. Res. Toxicol. Environ. Mutagen. 564, 9–20. http://dx.doi.org/10.1016/j.mrgentox.2004.06.010.
Martins, G.V., Marques, A.C., Fortunato, E., Sales, M.G.F., 2016. 8-hydroxy-2′-deoxyguanosine (8-OHdG) biomarker detection down to picoMolar level on a plastic antibody film. Biosens. Bioelectron. 86, 225–234. http://dx.doi.org/10.1016/j.bios.2016.06.052.
Martins, G.V., Tavares, A.P.M., Fortunato, E., Sales, M.G.F., 2017. Paper-based sensing device for electrochemical detection of oxidative stress biomarker 8-hydroxy-2′-deoxyguanosine (8-OHdG) in point-of-care. Sci. Rep. 7, 1–10. http://dx.doi.org/10.1038/s41598-017-14878-9.
Morioku, K., Morimoto, N., Takeuchi, Y., Nishina, Y., 2016. Concurrent formation of carbon–carbon bonds and functionalized graphene by oxidative carbon-hydrogen coupling reaction. Sci. Rep. 6, 25824. http://dx.doi.org/10.1038/srep25824.
Nishikawa, T., Sasahara, T., Kiritoshi, S., Sonoda, K., Senokuchi, T., Matsuo, T., Kukidome, D., Wake, N., Matsumura, T., Miyamura, N., Sakakida, M., Kishikawa, H., Araki, E., 2003. Evaluation of urinary 8-hydroxydeoxy-guanosine as a novel biomarker of macrovascular complications in type 2 diabetes. Diabetes Care 26, 1507–1512.
Otari, S.V., Kumar, M., Anwar, M.Z., Thorat, N.D., Patel, S.K.S., Lee, D., Lee, J.H., Lee, J.-K., Kang, Y.C., Zhang, L., 2017. Rapid synthesis and decoration of reduced graphene oxide with gold nanoparticles by thermostable peptides for memory device and photothermal applications. Sci. Rep. 7, 10980. http://dx.doi.org/10.1038/s41598-017-10777-1.
Rosy, Goyal, R.N., 2016. Determination of 8-Hydroxydeoxyguanosine: a potential biomarker of oxidative stress, using carbon-allotropic nanomaterials modified glassy carbon sensor. Talanta 161, 735–742. http://dx.doi.org/10.1016/j.talanta.2016.09.038.
Saravanabhavan, G., Blais, E., Vincent, R., Kumarathasan, P., 2010. A high performance liquid chromatography-electrochemical array method for the measurement of oxidative/nitrative changes in human urine. J. Chromatogr. A 1217, 3269–3274. http://dx.doi.org/10.1016/j.chroma.2010.01.048.
Shahzad, F., Zaidi, S.A., Koo, C.M., 2017a. Highly sensitive electrochemical sensor based on environmentally friendly biomass-derived sulfur-doped graphene for cancer biomarker detection. Sens. Actuators B Chem. 241, 716–724. http://dx.doi.org/10.1016/j.snb.2016.10.144.
Shahzad, F., Zaidi, S.A., Koo, C.M., 2017b. Highly sensitive electrochemical sensor based on environmentally friendly biomass-derived sulfur-doped graphene for cancer biomarker detection. Sens. Actuators B Chem. 241, 716–724. http://dx.doi.org/10.1016/j.snb.2016.10.144.
Shang, T., Wang, P., Liu, X., Jiang, X., Hu, Z., Lu, X., 2018a. Facile synthesis of porous single-walled carbon nanotube for sensitive detection of 8-Hydroxy-2′-deoxyguanosine. J. Electroanal. Chem. 808, 28–34. http://dx.doi.org/10.1016/j.jelechem.2017.11.064.
Shang, T., Wang, P., Liu, X., Jiang, X., Hu, Z., Lu, X., 2018b. Facile synthesis of porous single-walled carbon nanotube for sensitive detection of 8-Hydroxy-2′-deoxyguanosine. J. Electroanal. Chem. 808, 28–34. http://dx.doi.org/10.1016/j.jelechem.2017.11.064.
Shimoda, R., Nagashima, M., Sakamoto, M., Yamaguchi, N., Hirohashi, S., Yokota, J., Kasai, H., 1994. Increased formation of oxidative DNA damage, 8-hydroxydeoxyguanosine, in human livers with chronic hepatitis. Cancer Res. 54, 3171–3172.
Tamae, K., Kawai, K., Yamasaki, S., Kawanami, K., Ikeda, M., Takahashi, K., Miyamoto, T., Kato, N., Kasai, H., 2009. Effect of age, smoking and other lifestyle factors on urinary 7-methylguanine and 8-hydroxydeoxyguanosine. Cancer Sci. 100, 715–721.
Tığ, G.A., 2017. Development of electrochemical sensor for detection of ascorbic acid, dopamine, uric acid and L-tryptophan based on Ag nanoparticles and poly(L-arginine)-graphene oxide composite. J. Electroanal. Chem. 807, 19–28. http://dx.doi.org/10.1016/J.JELECHEM.2017.11.008.
Wang, Y., Li, J., Liu, Y., Ma, R., Jia, W., Cui, H., Wang, H., 2009. Fabrication of the DNA/poly(3-methylthiophene) composite film modified electrode and its application for the study on the voltammetric behavior and determination of 8-hydroxy-2′-deoxyguanosine. Sci. China Ser. B Chem. 52, 2006–2012. http://dx.doi.org/10.1007/s11426-009-0241-6.
Weiss, D.J., Lunte, C.E., 2000. Detection of a urinary biomaker for oxidative DNA damage 8-hydroxydeoxyguanosine by capillary electrophoresis with electrochemical detection. Electrophoresis 21, 2080–2085. http://dx.doi.org/10.1002/1522-2683(20000601)21:10<2080::AID-ELPS2080>3.0.CO;2-6.
Yang, L., Wang, B., Qi, H., Gao, Q., Li, C., Zhang, C., 2015a. Highly sensitive electrochemical sensor for the determination of 8-Hydroxy-2'-deoxyguanosine incorporating SWCNTs-Nafion composite film. J. Sens. 2015. http://dx.doi.org/10.1155/2015/504869.
Yang, L., Wang, B., Qi, H., Gao, Q., Li, C., Zhang, C., 2015b. Highly sensitive electrochemical sensor for the determination of 8-hydroxy-2′-deoxyguanosine incorporating SWCNTs-Nafion composite film. J. Sens. 2015, 1–11. http://dx.doi.org/10.1155/2015/504869.
Yi, Y., Zhu, G., Wu, X., Wang, K., 2016. Highly sensitive and simultaneous electrochemical determination of 2-aminophenol and 4-aminophenol based on poly(L-arginine)-β-cyclodextrin/carbon nanotubes@graphene nanoribbons modified electrode. Biosens. Bioelectron. 77, 353–358. http://dx.doi.org/10.1016/j.bios.2015.09.052.
Zhou, X., Jing, W., Zhuang, Z., Zheng, X., 2015. In situ synthesis of gold nanoparticles on poly (L-arginine) modified glassy carbon electrode and electrocatalytic oxidation of glucose in alkaline solution. ECS Electrochem. Lett. 4, G5–G7. http://dx.doi.org/10.1149/2.0071508eel.